*Proceedings of the*
*Annual Stability Conference*
*Structural Stability Research Council*
*Orlando, Florida, April 12-15, 2016*

# Quantitative Determination of Elastic Buckling Modes for Cold-Formed Steel Members

Robert S. Glauz, P.E.[1]

**Abstract**
The design of cold-formed steel members must consider a variety of buckling failure modes, including local buckling, distortional buckling, and global buckling. In 2004, the American Iron and Steel Institute incorporated the Direct Strength Method (DSM) into the North American Specification for the Design of Cold-Formed Steel Members as an alternative to traditional design methods. This method involves an elastic buckling analysis to determine buckling modes and stresses, and utilizes a series of nominal strength curves for predicting member strength. However, the strength curve selection requires mode determination based on general guidelines and interpretation of mode shapes. The purpose of this paper is to present a newly developed quantitative method of determining buckling modes. This will allow the complete DSM strength calculations to be performed by computer software without user intervention, and will enable stronger adoption of the Direct Strength Method.

## 1. Introduction

The Direct Strength Method (DSM) has been available for engineers to use with cold-formed steel design since the American Iron and Steel Institute (AISI) incorporated this option into the 2004 Edition of the Specification. This method is general in nature and offers some nice advantages, such as the ability to handle unconventional shapes.

The adoption of this method in the industry has been slow. This can be attributed to a number of factors relating to the time and effort involved. Specialized software is required to perform the elastic buckling analysis, effort is required to set up the analysis problem, calculation time inhibits iterative design changes, and the interpretation of buckling modes is a manual process.

Strides have been made in the availability of software, analysis setup effort, and calculation times. But the determination of buckling modes without user interpretation has not yet been accomplished. That is the objective of this paper.

[1] President/Owner, RSG Software, Inc., glauz@rsgsoftware.com

## 2. Buckling Modes

The DSM strength curves are defined for specific buckling modes: local buckling, distortional buckling, and global buckling. Figures 1 and 2 show the relationship between elastic buckling strength and nominal design strength for compression and bending, respectively.

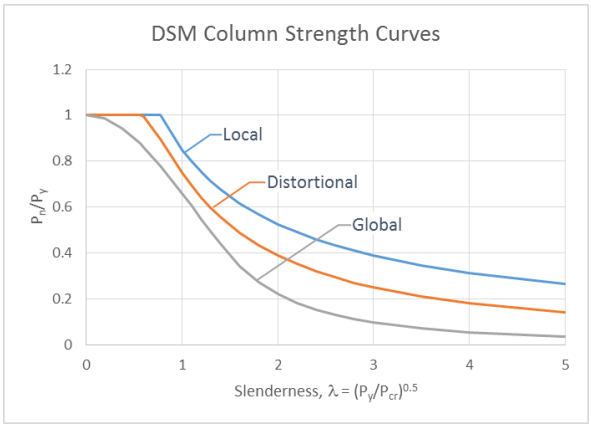


Figure 1

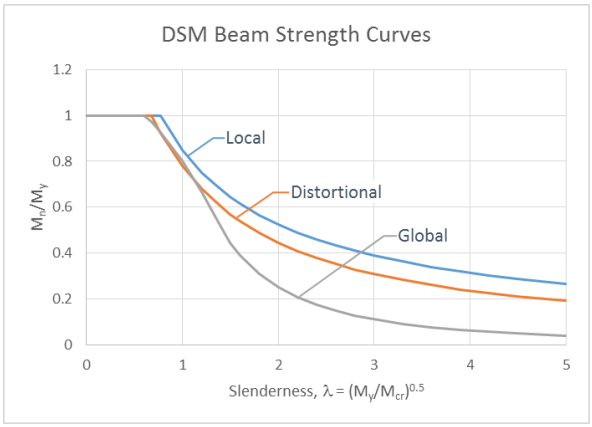


Figure 2

Local buckling involves the deformation of flat plate elements. It has significant post-buckling strength because much of the cross section remains substantially intact and is capable of carrying additional load. Distortional buckling has more section deformation and therefore the post buckling strength is lower. Global buckling can be either flexural, torsional, or flexural-torsional buckling. These global modes represent a limit state and there is no post-buckling strength.

For the direct strength method, it is important to correctly identify the buckling mode to utilize the appropriate strength curve. The DSM curves also incorporate interaction between local and global buckling, therefore proper distinction between local and distortional buckling is necessary.

For basic shapes, the definition of local and distortional buckling is well defined and illustrated with examples such as those in Figures 3 and 4 (AISI 2012b).

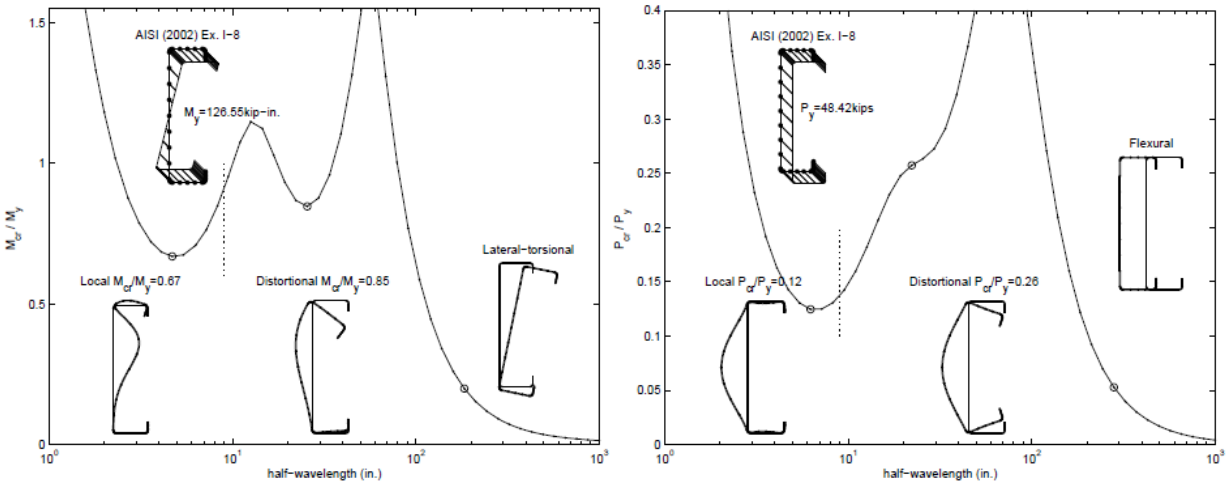


Figure 3: Example I-8 (AISI 2002)

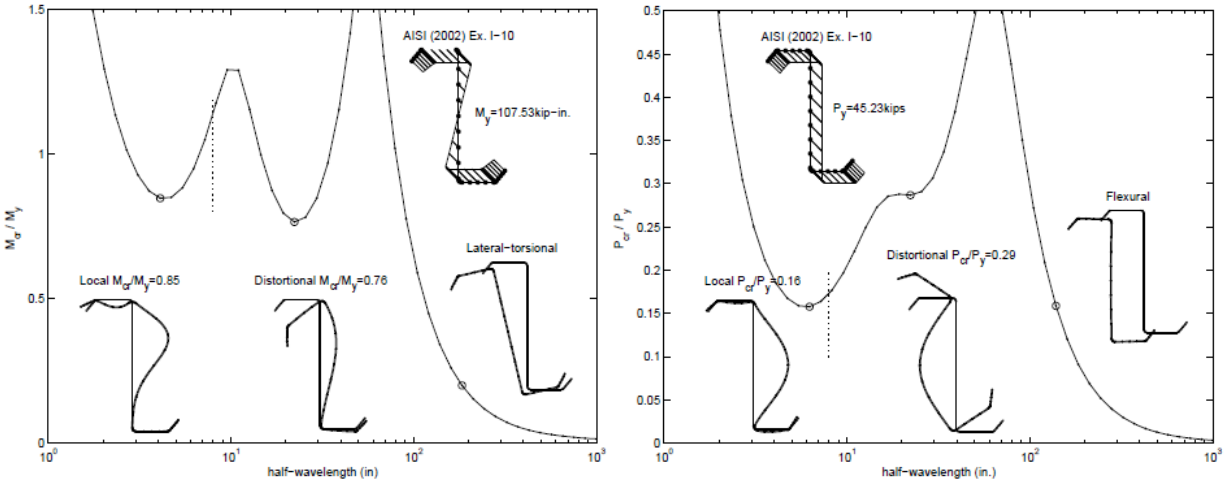


Figure 4: Example I-10 (AISI 2002)

For non-standard or more complex shapes, the mode determination may be less obvious and perhaps even a combination of modes. Figure 5 shows some example buckling modes which are more difficult to categorize.

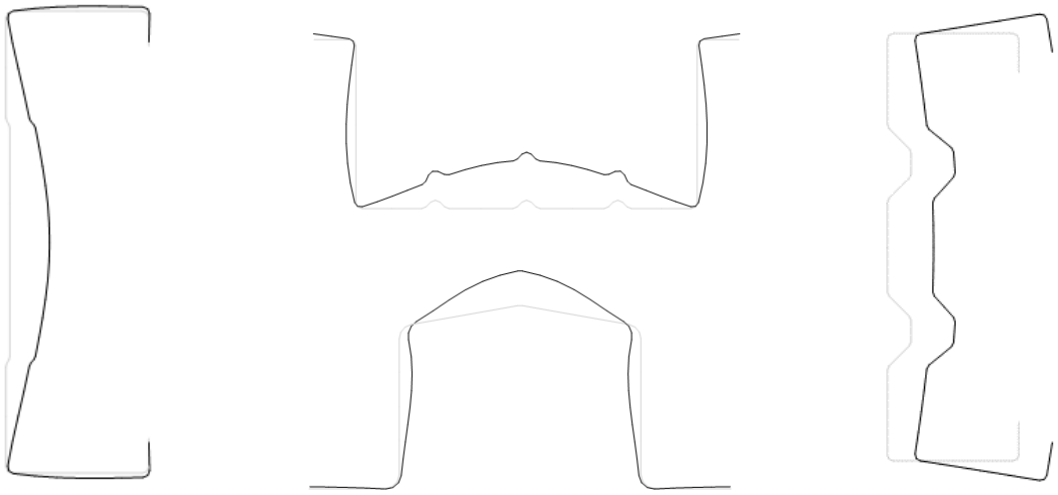

Figure 5

## 3. Quantitative Approach

The Commentary on North American Cold-Formed Steel Specification (AISI 2012b) provides a guideline for treating a buckling mode as local buckling where the half-wavelength is less than the largest characteristic dimension of the cross section. Larger half-wavelengths would be characterized as distortional buckling or global buckling.

For non-standard shapes it may not be evident how the largest characteristic dimension is defined. Another macro-level approach would be limits on $L/r_c$, where $r_c$ is the radius of gyration about the centroid. Preliminary study shows that $L/r_c < 3.5$ is generally local buckling, and $3.5 < L/r_c < 20$

is generally distortional buckling. However these are not definitive measures. They do not take into account the specific geometry of the cross section and the type of buckling deformation that occurs.

A micro-level approach that considers the section deformation is sensible to pursue. It was observed that variation in finite strip nodal rotations relative to nodal translations often provides a reliable differentiation of the different buckling modes. A standard deviation calculation was developed as shown in Equation 1.

$$s = \frac{\sqrt{\sum \varphi^2/n - (\sum \varphi/n)^2}}{\sum \delta / \sum w} \tag{1}$$

where:

$\varphi$ = rotation of each node
$\delta$ = translation of each node
$n$ = number of nodes
$w$ = width of each strip/element

An analysis of several different shapes showed that distortional buckling modes resulted in values of $s$ in the range of 0.1 to 0.5. Local buckling modes exhibited higher values, and global buckling modes resulted in lower values which approached zero as member length increased.

This demonstrates that a numerical evaluation is capable of reflecting characteristics of the buckled shape. However, this heuristic approach relies on statistical measures that do not properly account for changes in node distribution, variations in element stiffness, unique boundary conditions, etc. It is necessary to capture the mechanics of the section deformation in a quantitative way.

Observation of the axial deformation associated with different mode shapes revealed additional characteristics about the buckling types. The example in Figure 6 shows that local buckling has little axial deformation, whereas distortional and global buckling exhibit relatively large axial deformations (warping). The axial deformations in Figure 6 have been magnified for clarity.

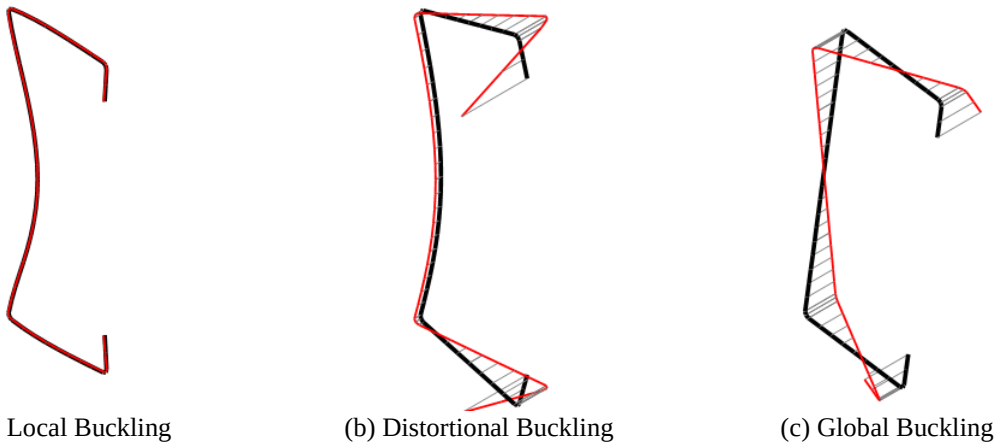

(a) Local Buckling (b) Distortional Buckling (c) Global Buckling

Figure 6

The mode shape deformation characteristics are summarized in Table 3.1 in a qualitative manner. The objective is to establish a quantitative measure of the section deformation and axial deformation.

Table 1: Buckling Characteristics

| Characteristic | Local | Distortional | Global |
|---|---|---|---|
| Section Deformation | Hi | Hi | Lo |
| Axial Deformation | Lo | Hi | Hi |

## 4. Work Method

A reasonable mechanical approach to measuring deformation is to calculate the work associated with the deformation for a specific mode shape. Local buckling involves more element curvature and therefore requires more section deformation work. Distortional buckling exhibits both section deformation and axial deformation, whereas global buckling has essentially no section deformation.

Mechanical work is determined by force applied and the distance moved by that force. In an elastic system the force increases with the amount of displacement. Figure 7 illustrates the example of a simple spring.

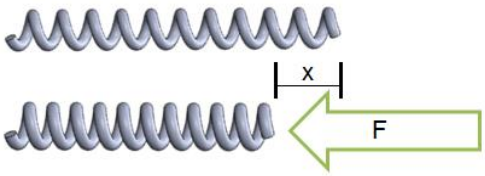


Figure 7

The force **F** is proportional to the displacement **x** by the spring constant **k** ($F = k \cdot x$). The work done by the force on the spring is determined as shown in Equation 2.

$$W = \int F \cdot dx = \int k \cdot x \cdot dx = \tfrac{1}{2} k x^2 \tag{2}$$

For a system with multiple degrees of freedom, the work done is expressed in matrix form as shown in Equation 3.

$$W = \tfrac{1}{2} \{d\}^T [K] \{d\} \tag{3}$$

where **{d}** (Nx1) represents displacements, and **[K]** (NxN) represents the elastic stiffness matrix. In an elastic buckling analysis for a specific half-wavelength, **[K]** and **{d}** are already determined. The mode shape displacements **{d}** for a finite strip analysis include four different directions for each node: horizontal (**x**), vertical (**y**), rotational (**θ**), and axial (**z**), as shown in Figure 8.

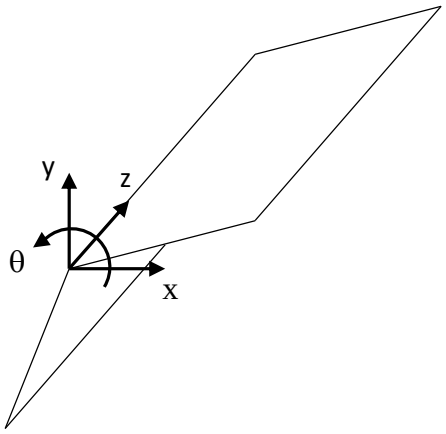


Figure 8

To calculate the work associated with the cross section deformation, it is necessary to separate the in-plane displacements, which involves directions x, y, and θ. However, these displacements may include global translation or rotation of the member (flexural or torsional buckling). To isolate the section deformation, these global displacements must be determined and subtracted from the total displacements.

The result is a section deformation matrix {ds} which is determined as follows for each node i:

$$d_{sxi} = d_{xi} - (\bar{x} - Y_i\bar{\theta}) \quad (4)$$

$$d_{syi} = d_{yi} - (\bar{y} + X_i\bar{\theta}) \quad (5)$$

$$d_{szi} = 0 \quad (6)$$

$$d_{s\theta i} = d_{\theta i} - \bar{\theta} \quad (7)$$

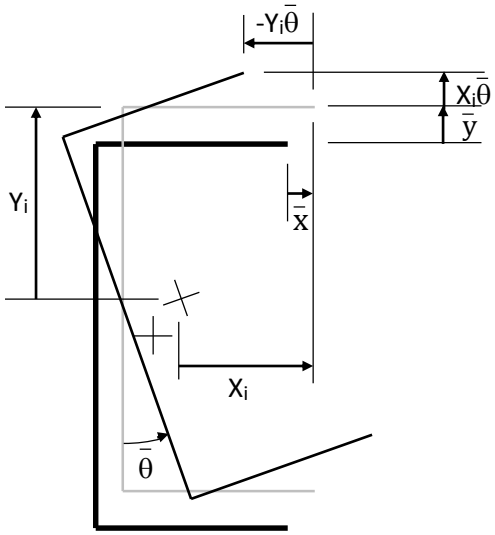


Figure 9

where these terms are illustrated in Figure 9 and defined as:

$\bar{x}$ = mean horizontal displacement

$\bar{y}$ = mean vertical displacement
$\bar{\theta}$ = mean rotational displacement
$X_i$ = horizontal coordinate of node from centroid
$Y_i$ = vertical coordinate of node from centroid

The work associated with the section deformation is then determined by:

$$W_s = \frac{1}{2} \{d_s\}^T [K] \{d_s\} \quad (8)$$

The scaling of the mode shape displacements is arbitrary, so a normalization of the deformation work is required. This is accomplished by dividing the *section* deformation work by the *axial* deformation work. The axial deformation work is calculated as:

$$W_a = \frac{1}{2} \{d_a\}^T [K] \{d_a\} \quad (9)$$

where $\mathbf{\{d_a\}}$ is developed as follows for each node i:

$$d_{axi} = 0 \quad (10)$$
$$d_{ayi} = 0 \quad (11)$$
$$d_{azi} = d_{zi} \quad (12)$$
$$d_{a\theta i} = 0 \quad (13)$$

Therefore, the normalized deformation work is the unitless ratio $W_s / W_a$. The magnitude of this ratio can vary greatly, so for convenience the work ratio is defined using the square root of the ratio as shown in Equation 14.

$$\lambda_w = \sqrt{W_s / W_a} \quad (14)$$

## 5. Results

Several example sections were analyzed using this work ratio calculation. For common local buckling modes, this ratio was generally in the range of 20 to 100. Distortional buckling values were typically between 2 and 10. Global buckling values approached 0 as expected, because the global displacements are subtracted to obtain the section deformations, and this buckling mode has essentially no section deformation.

Figures 10 through 18 on the following pages contain plots of the elastic buckling stress profiles (in blue) and the corresponding section deformation work ratios (in red).

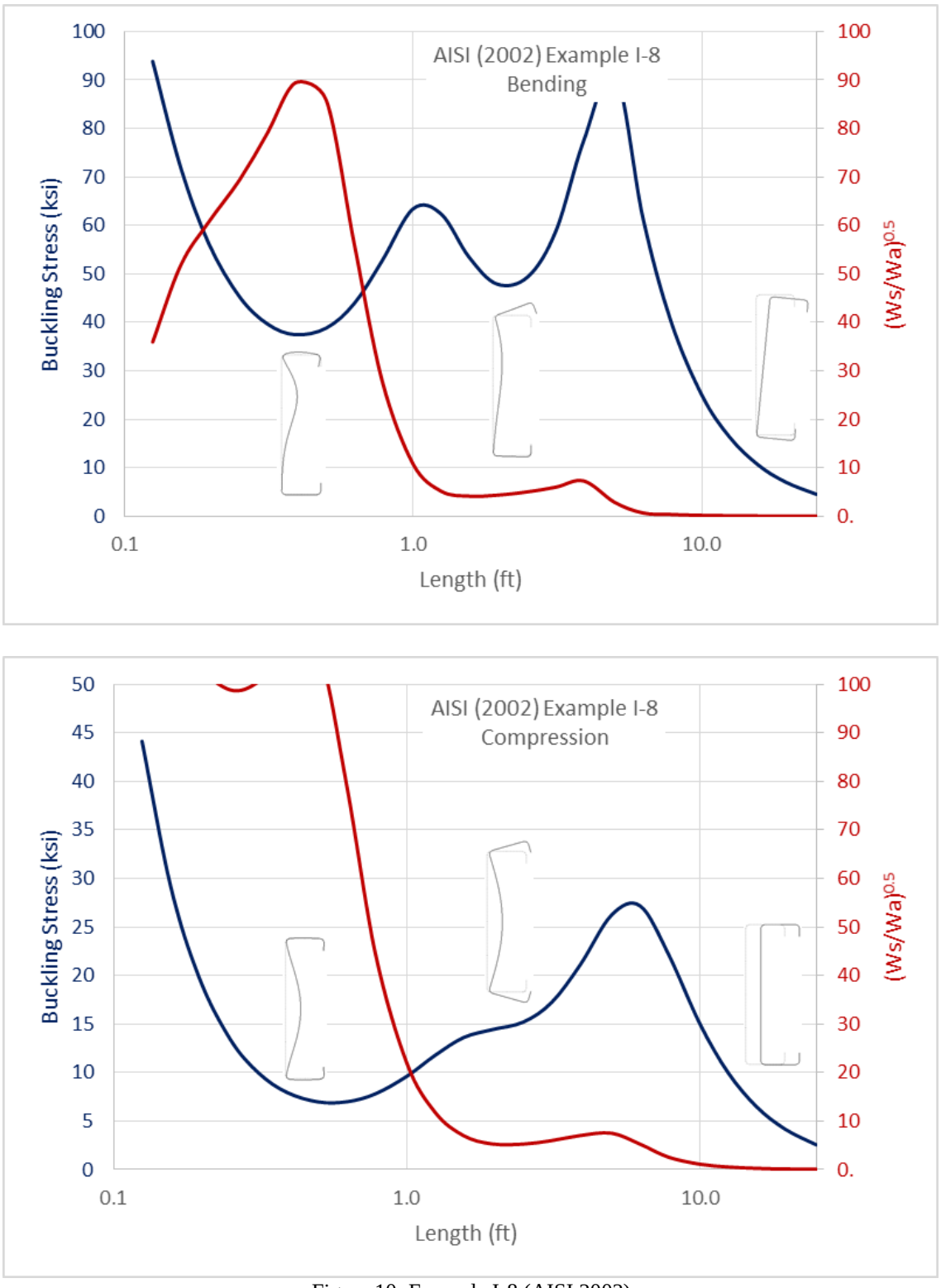


Figure 10: Example I-8 (AISI 2002)

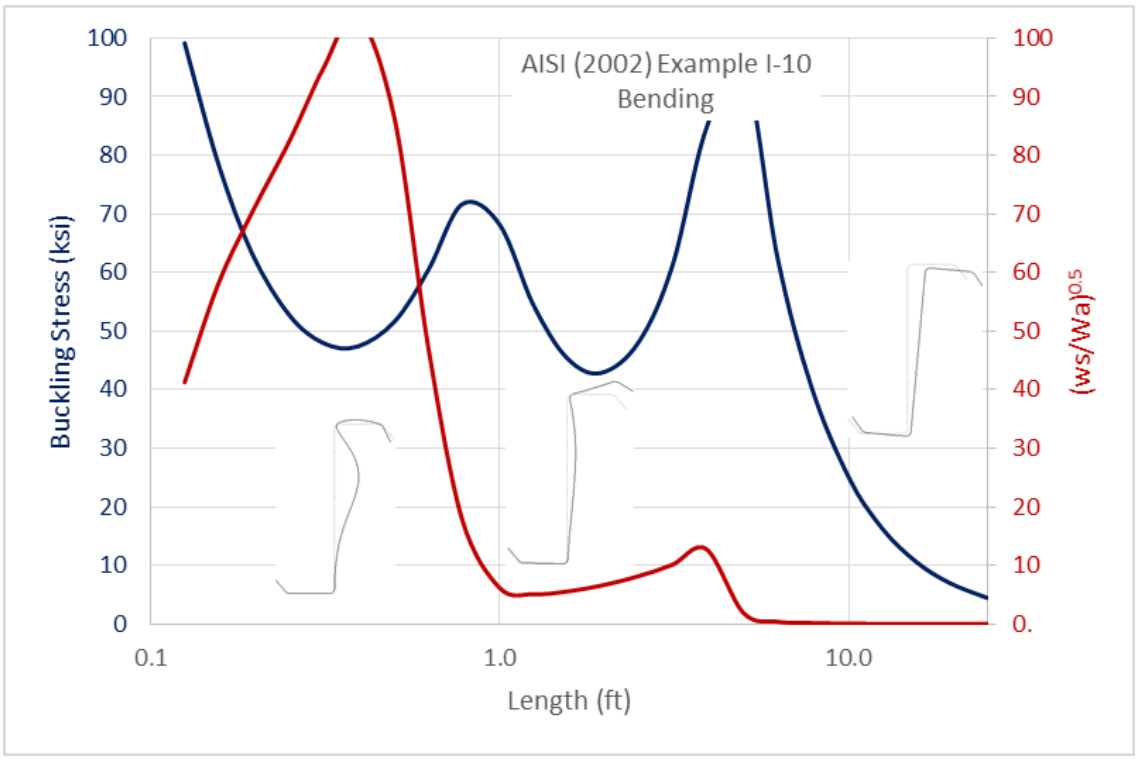


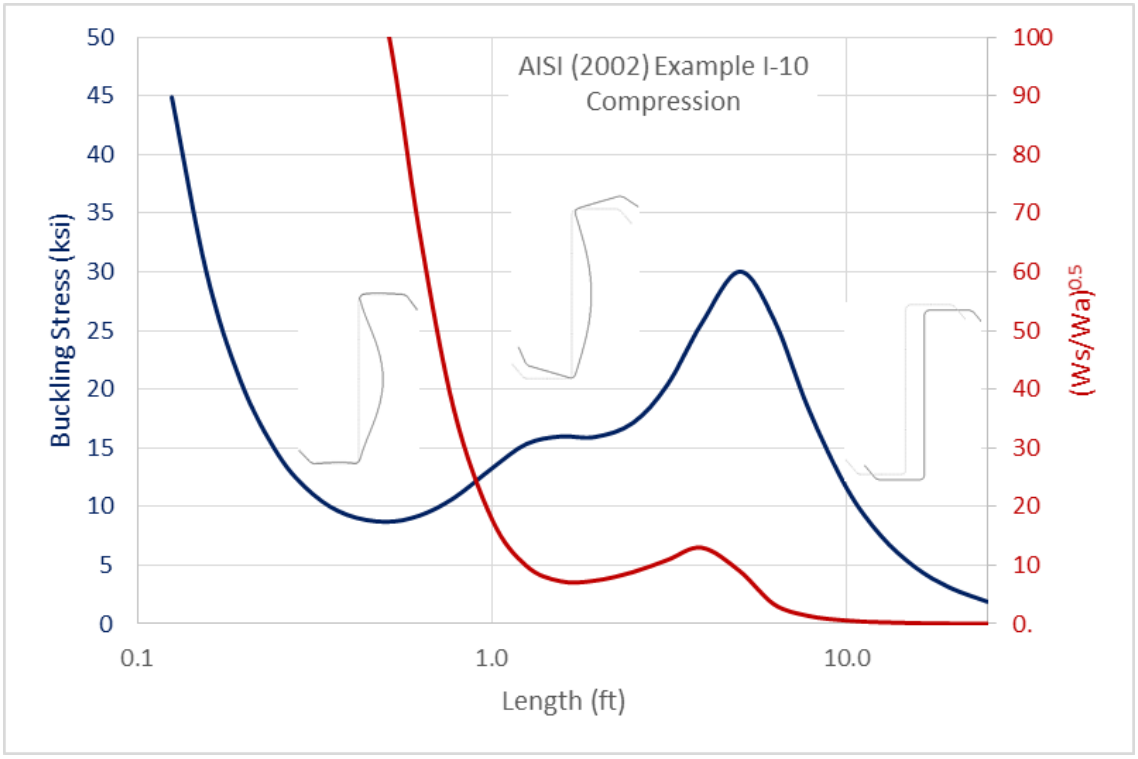


Figure 11: Example I-10 (AISI 2002)

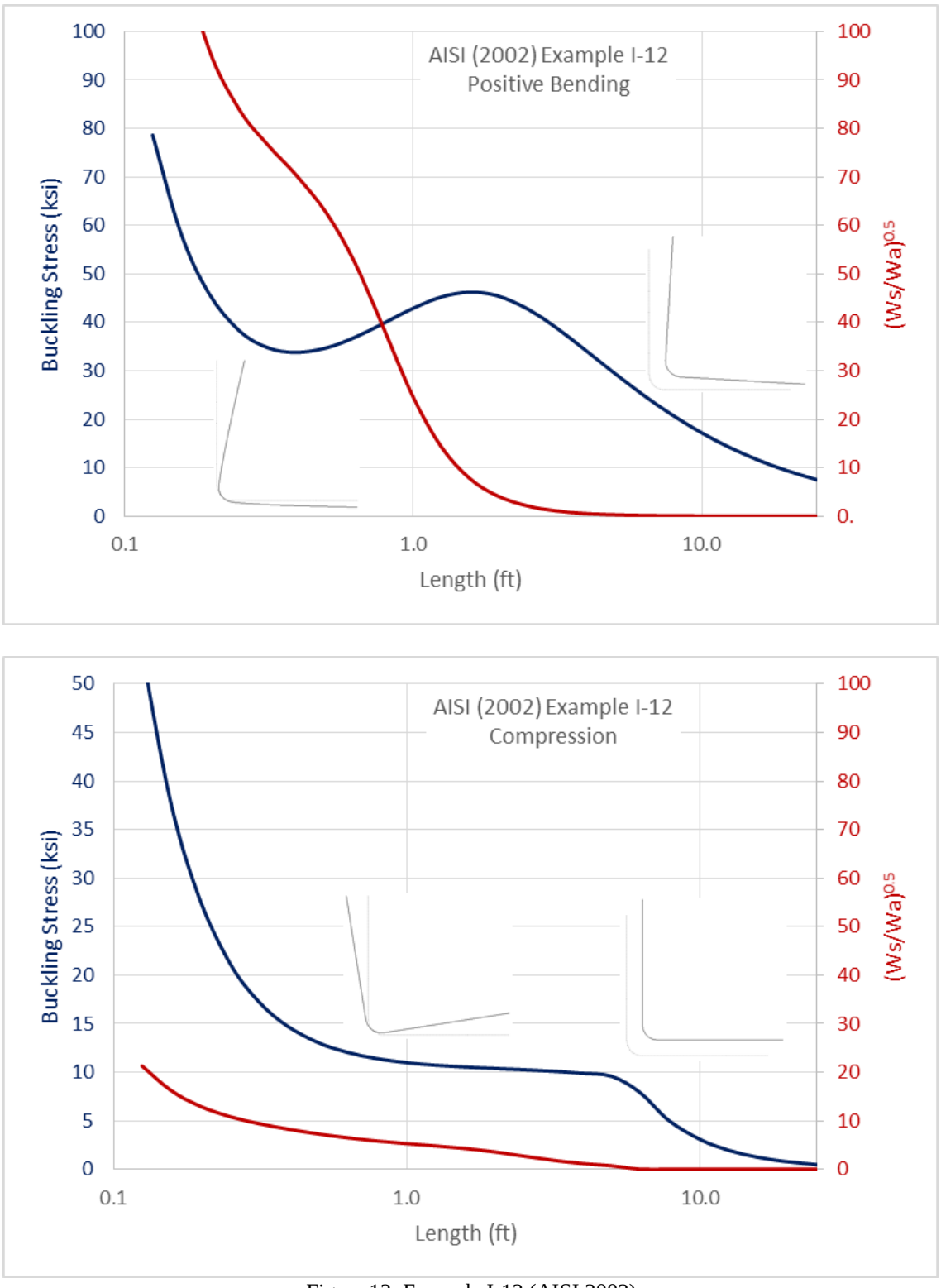


Figure 12: Example I-12 (AISI 2002)

Figure 12 illustrates that the first mode for bending is categorized as local buckling (high work ratio), whereas the first mode for compression is categorized as distortional buckling (low work ratio).

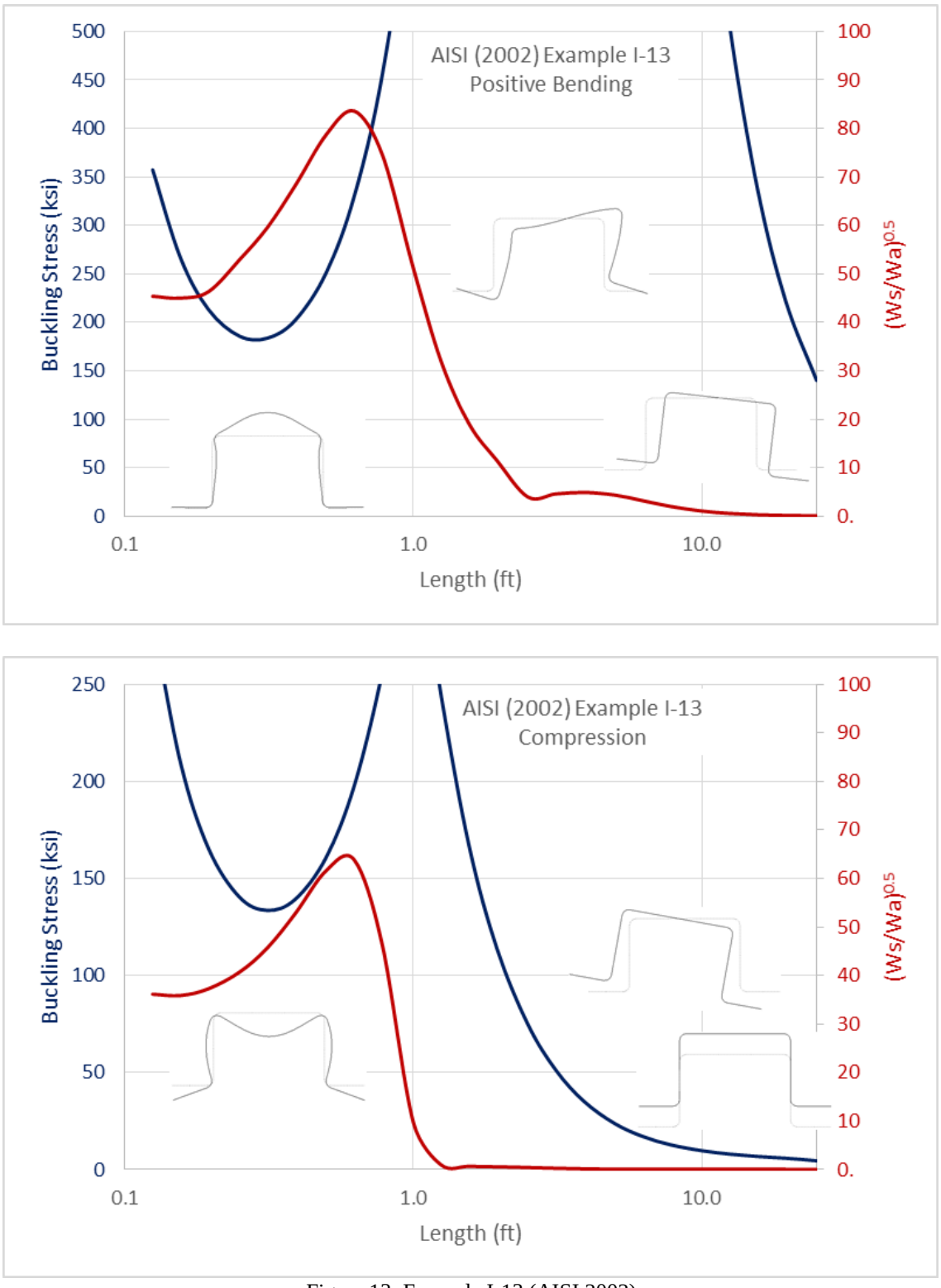


Figure 13: Example I-13 (AISI 2002)

For the hat shape in bending shown in Figure 13, the distortional buckling mode between 3 ft and 10 ft does not have any stress minima. For the compression case, global buckling experiences torsion and flexure at different lengths.

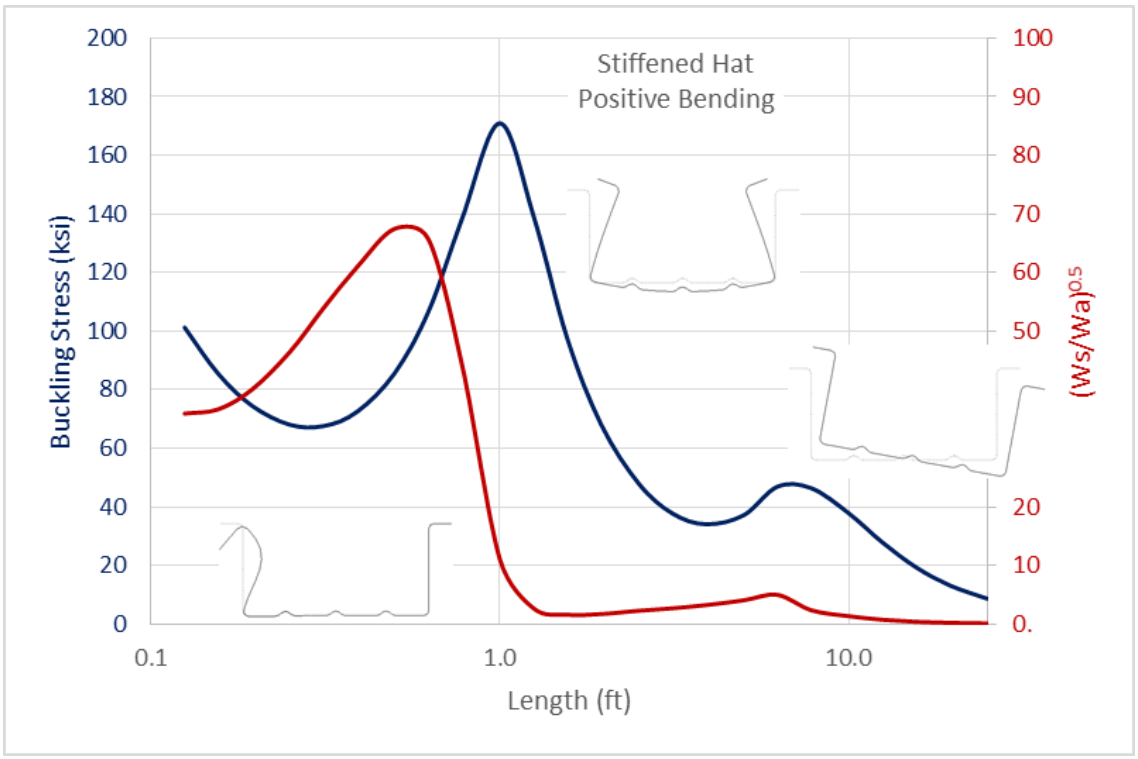


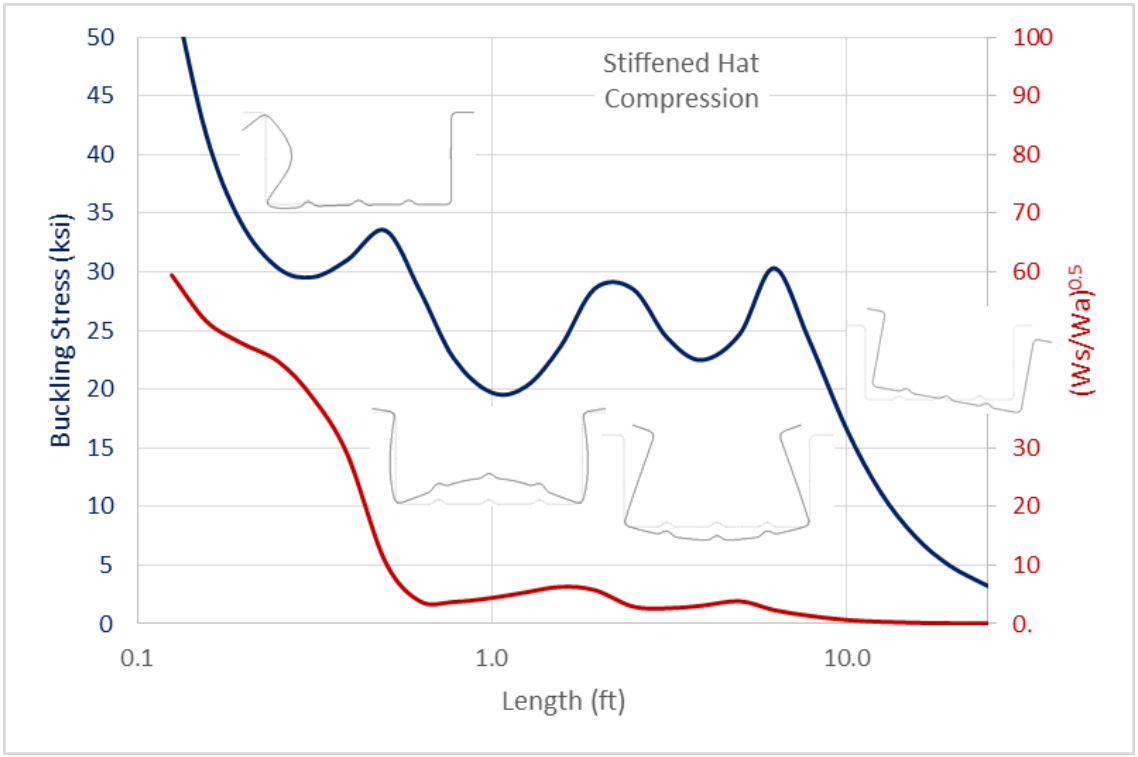


Figure 14: Hat with Intermediate Stiffeners

For the compression case shown in Figure 14, this shape experiences two distinct distortional buckling modes at different lengths.

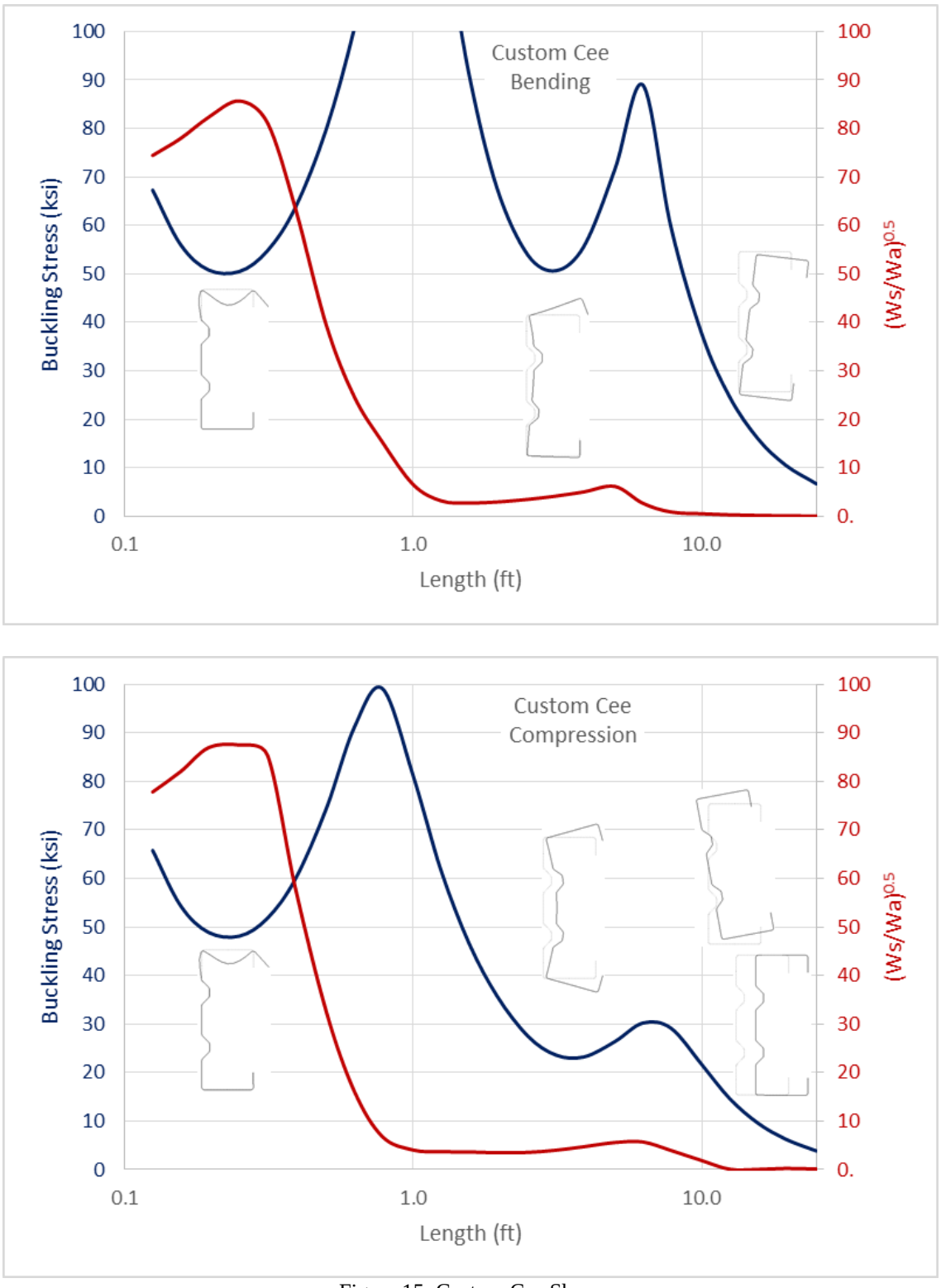


Figure 15: Custom Cee Shape

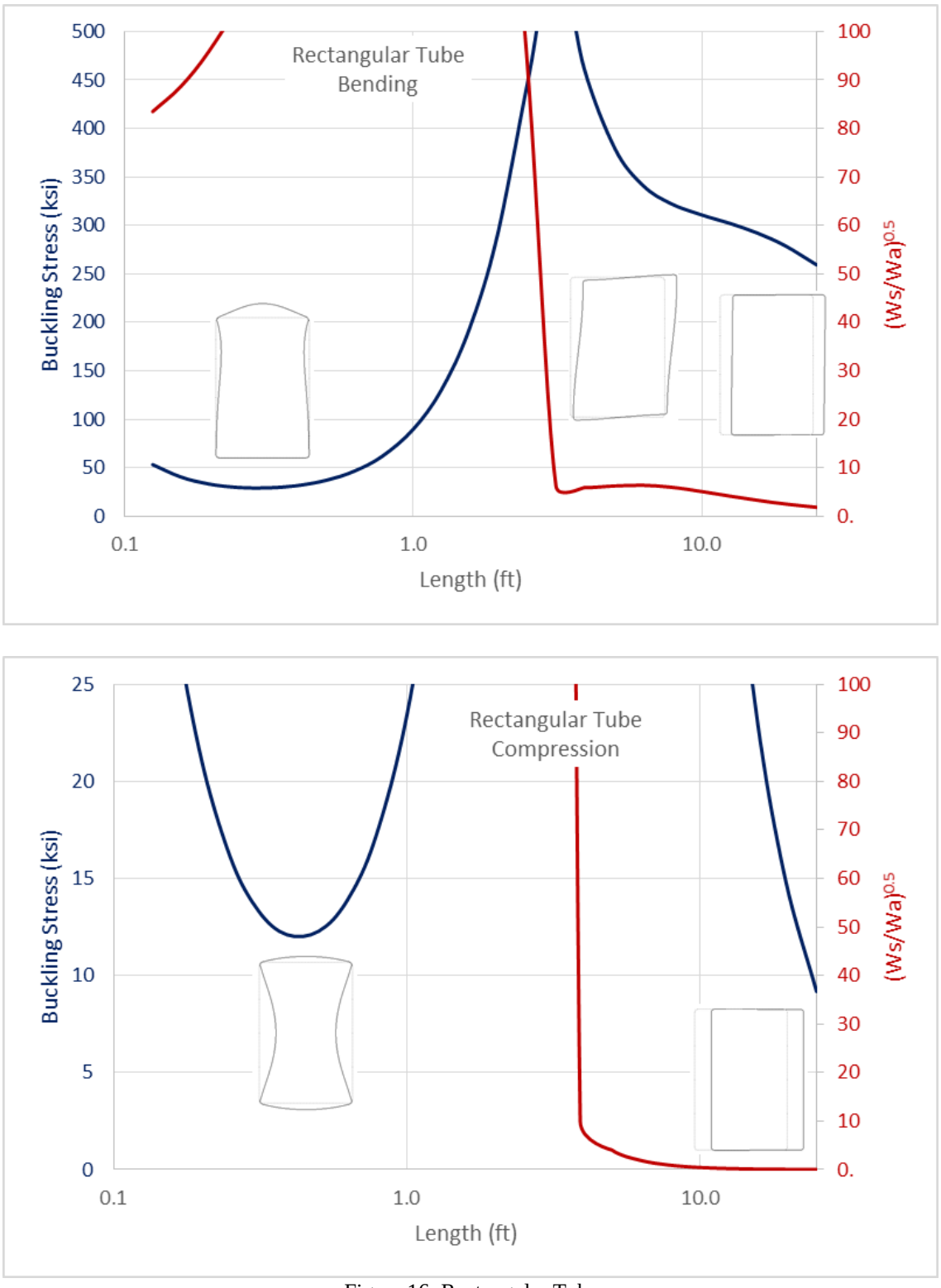


Figure 16: Rectangular Tube

For the rectangular tube in bending shown in Figure 16, the distortional buckling mode between 5 ft and 20 ft, does not have any stress minima.

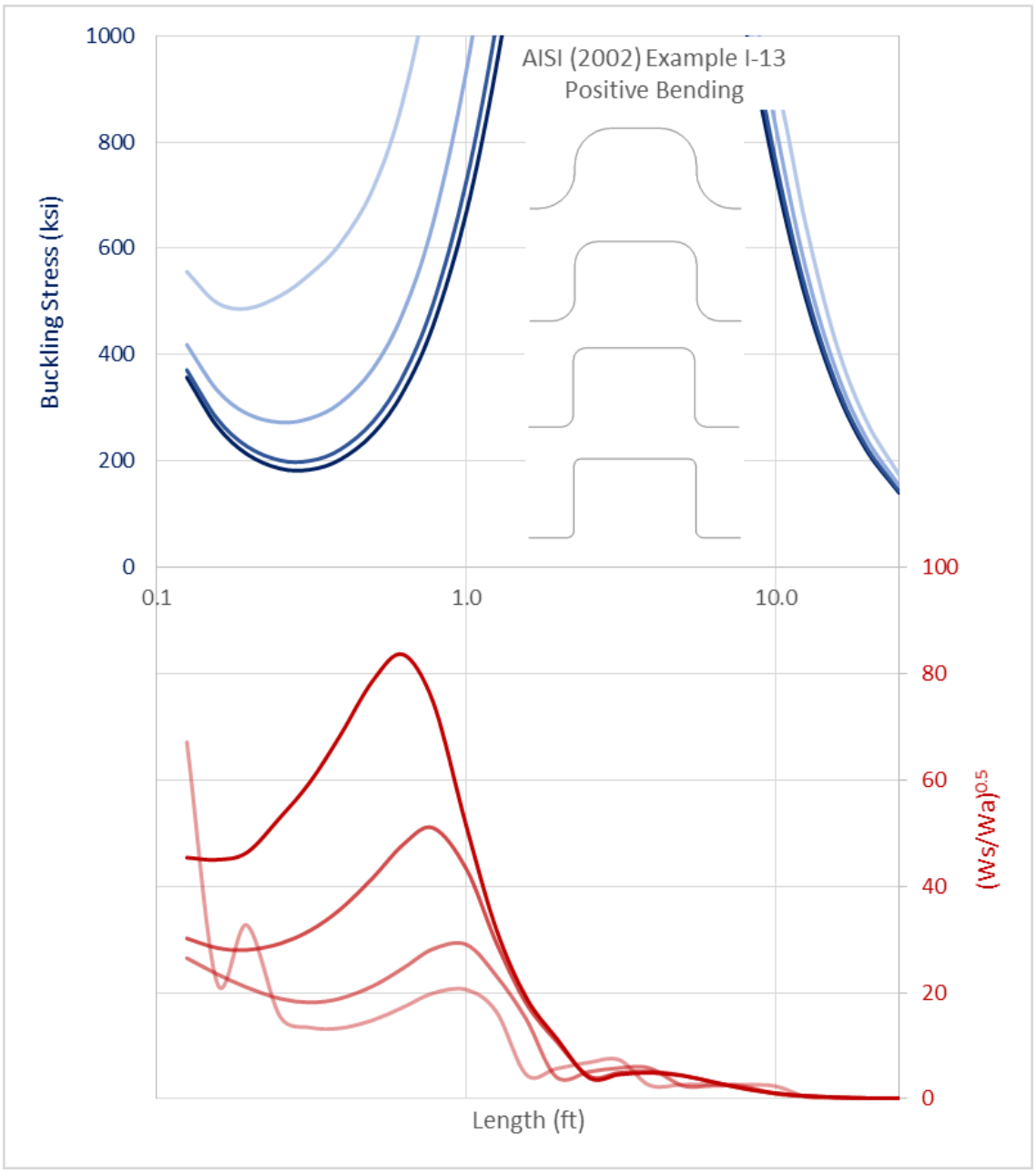


Figure 17: Bend Radius Impact

Figure 17 demonstrates that as the bend radius increases, the work ratio decreases but the buckling mode remains local buckling. Lengths between 2 and 10 ft experience distortional buckling (as in Figure 13), but no stress minima exist.

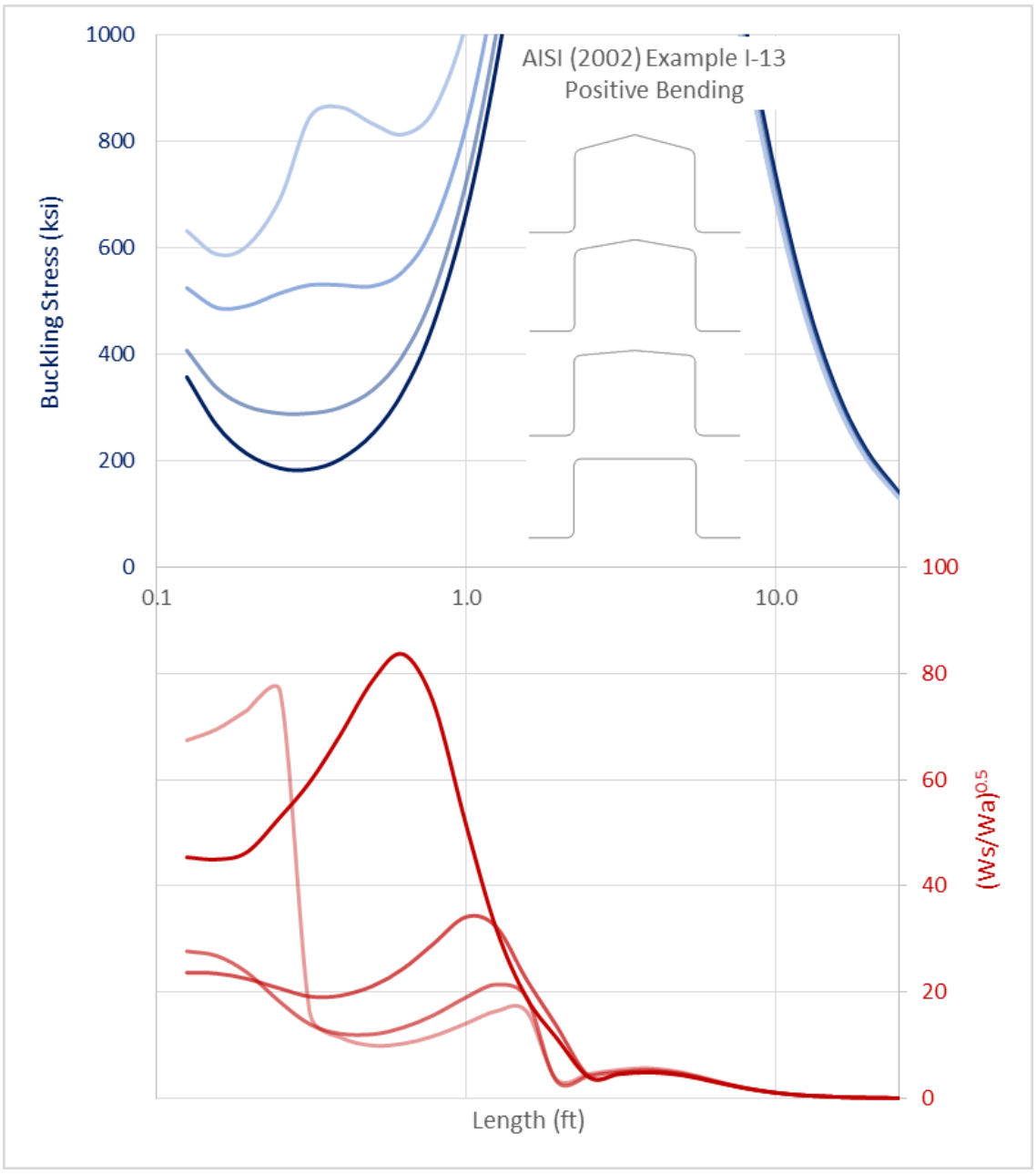


Figure 18: Bent Flange Impact

For a hat shape in positive bending, Figure 18 shows the introduction of a bent top flange at angles of 5, 10, and 15 degrees. This increases the buckling stress and decreases the work ratio. For the 10 and 15 degree flange angles, two stress minima occur, one as local buckling and one as distortional buckling.

## 6. Conclusions

With current descriptive characterizations of mode shapes, some buckling modes may be indistinct or difficult to establish. The work method presented in this paper typically depicts a distinct difference between local buckling and distortional buckling, and between distortional buckling and global buckling. Furthermore, the local and distortional buckling stress minima generally fall between the abrupt changes in the work ratio.

The elegance of this method is that no assumptions about the section geometry or the analysis model are required. If the model is sufficient to provide elastic buckling values and mode shapes, it can also be used to reliably categorize buckling modes, whether the section consists of flat elements, stiffened elements, curved elements, or unconventional shapes.

The simplicity of this approach is evident from its use of the elastic stiffness matrix and mode shape displacements already determined in the elastic buckling analysis. The displacement adjustments and subsequent matrix multiplications require little computational effort.

The recommendation is that section deformation work ratios, $\lambda_w$, between 1 and 16 should be treated as distortional buckling, higher values should be treated as local buckling, and lower values should be treated as global buckling. Suitable language for this approach will be proposed to the American Iron and Steel Institute for inclusion in the next edition of the North American Specification for the Design of Cold-Formed Steel Structural Members.

## References


American Iron and Steel Institute (2002), *Cold-Formed Steel Design Manual*, Washington, DC, 2002.

American Iron and Steel Institute (2012a), *North American Specification for the Design of Cold-Formed Steel Structural Members*, Washington, DC, 2012.

American Iron and Steel Institute (2012b), *Commentary on North American Specification for the Design of Cold-Formed Steel Structural Members*, Washington, DC, 2012.

Wang, C. K. (1970), *Matrix Methods of Structural Analysis*, Second Edition, American Publishing Co., Madison, WI, 1970.